THE JOURNAL OF BIOLOGICAL CHEMISTRY VOL. 291, NO. 7, pp. 3395–3410, February 12, 2016

Rapid Activation of Bone Morphogenic Protein 9 by Receptor-mediated Displacement of Pro-domains*

Received for publication, August 6, 2015, and in revised form, December 14, 2015 Published, JBC Papers in Press, December 16, 2015, DOI 10.1074/jbc.M115.680009

Yvonne Kienast[‡§1], Ute Jucknischke[‡§], Stefan Scheiblich[‡§], Martina Thier[‡¶], Mariana de Wouters[‡¶], Alexander Haas[‡‖], Christian Lehmann[‡§], Verena Brand[‡], Dirk Bernicke[‡§], Konrad Honold[‡§], and Stefan Lorenz[‡‖]

From the [‡]Roche Pharma Research and Early Development (pRED), [§]Discovery Oncology, Roche Innovation Center Penzberg, 82377 Penzberg, Germany, [¶]Translational Technologies and Bioinformatics, Roche Innovation Center, Basel, 4070 Basel, Switzerland, and [‖]Large Molecule Research, Roche Innovation Center Penzberg, 82377 Penzberg Germany

By non-covalent association after proteolytic cleavage, the pro-domains modulate the activities of the mature growth factor domains across the transforming growth factor-β family. In the case of bone morphogenic protein 9 (BMP9), however, the pro-domains do not inhibit the bioactivity of the growth factor, and the BMP9·pro-domain complexes have equivalent biological activities as the BMP9 mature ligand dimers. By using real-time surface plasmon resonance, we could demonstrate that either binding of pro-domain-complexed BMP9 to type I receptor activin receptor-like kinase 1 (ALK1), type II receptors, co-receptor endoglin, or to mature BMP9 domain targeting antibodies leads to immediate and complete displacement of the pro-domains from the complex. Vice versa, pro-domain binding by an anti-pro-domain antibody results in release of the mature BMP9 growth factor. Based on these findings, we adjusted ELISA assays to measure the protein levels of different BMP9 variants. Although mature BMP9 and inactive precursor BMP9 protein were directly detectable by ELISA, BMP9·pro-domain complex could only be measured indirectly as dissociated fragments due to displacement of mature growth factor and pro-domains after antibody binding. Our studies provide a model in which BMP9 can be readily activated upon getting into contact with its receptors. This increases the understanding of the underlying biology of BMP9 activation and also provides guidance for ELISA development for the detection of circulating BMP9 variants.

Bone morphogenic protein 9 (BMP9[2]; also known as growth and differentiation factor 2 (GDF2)), is a member of the transforming growth factor β (TGFβ) superfamily. BMP9 is constitutively expressed in liver and secreted into the circulation at active concentrations (1). Circulating BMP9 is a potent biological effector signaling through type I receptor activin-receptor-like kinase 1 (ALK1) in endothelial cells, thereby maintaining vascular homeostasis (2, 3). BMP9 and ALK1 are required for properly organized blood and lymphatic vascular development (4–6). Human mutations in ALK1 lead to a genetic vascular disorder known as hereditary hemorrhagic telangiectasia (7). Recently, mutations in BMP9 have been identified in individuals with a vascular disorder phenotypically overlapping with hereditary hemorrhagic telangiectasia (8). BMP9 was also discovered to function as a neurotropic factor, potently inducing and maintaining the cholinergic phenotype in the central nervous system (9), and is also the most potent BMP for inducing osteogenic, and to a lesser extent adipogenic and chondrogenic differentiation (10, 11). Osteogenic signaling requires both ALK1 and the low affinity type I receptor ALK2 (12). Type II receptors activin receptor IIA and IIB (ActRIIA and ActRIIB) and BMP receptor II (BMPRII) have also been implicated in ALK1/BMP9 signaling (13). Moreover, endoglin (ENG) has been identified as a co-receptor that can increase BMP9/ALK1 signaling (3, 14). This is reflected in a model where ENG and ALK1 act together to bind and capture BMP9 on the cell surface. The type II receptors then function to displace the bound ENG to form a type I/type II receptor signaling complex.

BMP9 is synthesized as a precursor protein that is enzymatically processed by pro-protein convertases (*e.g.* furin; Ref. 1) in the *trans*-Golgi network, generating an N-terminal pro-domain (amino acids 23–319) and a C-terminal disulfide cross-linked mature dimer (amino acids 320–429). The secreted form of BMP9 is a complex (hereinafter referred to as BMP9·pro-domain) consisting of the mature BMP9 dimer and two non-covalently associated pro-domains. There is increasing evidence that the pro-domains contribute to the tremendous functional diversity among the 33 members of the TGFβ family (15–17). For example, the pro-domains of TGFβ, the prototype member of the family, target the growth factor to the extracellular matrix and confer latency to the growth factor dimer (15). Significant structural rearrangements have been shown to occur when the pro-domain of TGFβ (called β1-latency-associated peptide or β1-LAP) forms a complex with TGFβ (15). Activation of TGFβ growth factor pro-domain complexes occurs through thrombospondin- and integrin-mediated mechanisms and proteolytic cleavage of the pro-domains (18–20). Despite structural similarity between BMP9 and TGFβ, bioactivity assays demonstrate equivalent biological activities for pro-domain-complexed BMP9 and the mature BMP9 ligand (21). In support of this recent studies deciphered the crystal structure

* Y. K., U. J., S. S., M. T., M. W., A. H., C. L., V. B., D. B., K. H., and S. L. (all authors) are employees of Roche Diagnostics GmbH.

[1] To whom correspondence should be addressed: Roche Pharma Research and Early Development, Discovery Oncology, Roche Innovation Center Penzberg, Roche Diagnostics GmbH, Nonnenwald 2, 82377 Penzberg, Germany. Tel.: 49-8856-60-6308; Fax: 49-8856-60-79-6308; E-mail: yvonne.kienast@roche.com.

[2] The abbreviations used are: BMP, bone morphogenic protein; BMPRII, BMP receptor II; Ab, antibody; SRP, surface plasmon resonance; GDF, growth and differentiation factor; ALK1, activin receptor-like kinase 1; ActRIIA and ActRIIB, activin receptor IIA and IIB; ECD, extracellular domain; ENG, endoglin; hu-, human.

of the BMP9·pro-domain complex, demonstrating an open-armed, non-latent conformation of BMP9·pro-domain that contrasts with the cross-armed, latent conformation of TGFβ·pro-domain (22).

To shed further light on the biological function of pro-domain-complexed BMP9, we investigated the dynamics of mature BMP9 or BMP9·pro-domain complex interactions with the major BMP9 receptor ALK1, type II receptors BMPRII, ActRIIA, ActRIIB, co-receptor ENG, or mature BMP9-domain targeting antibodies by real-time surface plasmon resonance (SPR). Our data reveal that only the mature BMP9 domain is able to bind to ALK1, BMPRII, ActRIIA, ActRIIB, and ENG and that the pro-domains are completely and rapidly displaced by the receptors or by BMP9 targeting antibodies. Vice versa, pro-domain binding by an anti-pro-domain antibody results in release of the mature BMP9 growth factor. Based on the molecular mechanisms described here, we supplemented previously developed enzyme-linked immunosorbent assays (ELISA) assays (1) to measure the protein levels of all different BMP9 variants. Although the mature BMP9 dimer and the inactive precursor protein were directly detectable by ELISA, BMP9·pro-domain complex could only be measured indirectly as dissociated fragments due to displacement of mature growth factor and pro-domains after antibody binding.

These studies provide a model for rapid activation of BMP9 in which all relevant receptors are able to completely displace the BMP9 pro-domains to activate the signaling process, thereby ensuring angiogenic balance. As BMP9-targeting antibodies can also compete with the pro-domains for binding to BMP9, our findings are of translational interest for ELISA development for the detection of different circulating BMP9 variants.

Experimental Procedures

Blood Donors—Human plasma from healthy individuals of Western European descent ($n = 17$) was obtained from Indivumed (Hamburg, Germany). Written informed consent was obtained from all individuals permitting the commercial use of donated blood samples. The study was approved by the Data Protection Authority Hamburg. Procedures in place respect the German data protection laws as well as United States regulations. Indivumed acts in strict compliance with The Declaration of Helsinki and The Convention on Human Rights and Biomedicine. Mouse blood was taken from 8–10-week-old female Balb/c mice into EDTA-coated tubes. Plasma was frozen until BMP9 ELISA measurements were performed. Mice were obtained from Charles River Laboratories and maintained under specific-pathogen-free conditions with daily cycles of 12-h light/12-h darkness. The taking of blood samples was conducted in accordance with committed guidelines (TierSchG; GV-Solas; Felasa) and was approved by the Animal Welfare Body of the Government of Upper Bavaria, Germany (approval number 55.2-1-54-2532.0-65-14). The animal facility is AAALAC (Association for Assessment and Accreditation of Laboratory Animal Care International)-accredited.

Antibodies and Recombinant Proteins—Antibodies used included anti-mature BMP9 antibodies MAB3209 and its biotinylated conjugate BAF3209 and anti-pro-domain antibodies AF3879 and its biotinylated conjugate BAF3879 and were purchased from R&D Systems. Anti-mature BMP9 mAb BMP9-0087 was generated at Roche Innovation Center Penzberg by rabbit immunization with full-length recombinant human BMP9. Roche monoclonal anti-IGF1R antibody (RO4858696) was used as a negative control for SPR analysis. Anti-ALK1antibody (RO6858077) was generated in-house based on the sequence of a previously reported therapeutic antibody candidate (23). Chimeric human BMPRII-Fc, ActRIIA-Fc, and ActRIIB-Fc were purchased from R&D Systems. The recombinant human free mature BMP9 protein was purchased from R&D Systems or manufactured in-house (see below).

Cloning and Purification of Recombinant BMP9 Variants and Pro-domain—BMP9·pro-domain (pro-domain amino acids 23–319, mature protein amino acids 320–429) DNA based on NCBI reference sequence NP_057288.1 was synthesized (Geneart, Regensburg, Germany) as cDNA, subcloned into expression vectors, and amplified in *Escherichia coli* XL1Gold (Invitrogen). The signal sequence (amino acids 1–22) was replaced by a murine leader peptide (MGW SCI ILF LVA TAT GVH S). In the precursor BMP9 construct, Arg-317 and Lys-318 were both replaced by Ala to inhibit proteolytic cleavage by convertases. Sequence integrity was confirmed by sequencing performed at Sequiserve GmbH (Vaterstetten, Germany). The plasmids were amplified in *E. coli*, purified, and subsequently applied for transient transfections of HEK293-F cells using the FreeStyle™ 293 Expression System according to the manufacturer's instruction (Invitrogen). The suspension FreeStyle 293-F cells was cultivated in FreeStyle 293 Expression medium at 37 °C and 8% CO_2; the cells were seeded in fresh medium at a density of $1–2 \times 10^6$ viable cells/ml on the day of transfection. The DNA-293·fectin complexes were prepared in Opti-MEM medium (Invitrogen) using 333 μl of 293 fectin and 500 μg of plasmid DNA in a 1:1 molar ratio for a final transfection volume of 250 ml. The cell culture supernatants were clarified 7 days after transfection by centrifugation at $14,000 \times g$ for 30 min and filtration through a sterile filter (0.22 μm). Supernatants were stored at −20 °C until they were purified as described (21). Monomer content and integrity of the proteins were confirmed by size exclusion-HPLC and capillary electrophoresis-SDS measurements. Mature BMP9 and pro-domains were isolated from pro-domain-complexed BMP9 by 50% cold ethanol precipitation as described (21).

Cloning and Purification of Recombinant Human ALK1-Fc and ENG-Fc—DNA stretches of interest (human ALK1 ECD Asp-22–Gln-118 and human ENG ECD Glu-26–Gly-586 followed by a Avi Tag and PreScission site fused to the Hinge Region of human IgG1) were synthesized (Geneart, Regensburg, Germany), subsequently subcloned into appropriate expression vectors, and amplified in *E. coli* XL1Gold (Invitrogen). In addition to the fusion protein expression cassette, the expression vector contained an origin of replication, a β-lactamase gene, the immediate early enhancer and promoter from the human cytomegalovirus (HCMV) and a BGH polyadenylation sequence. The fusion protein was coded as cDNA sequences and synthesized with a 5′-end DNA sequence coding for a leader peptide (MGW SCI ILF LVATAT GVH S) to target proteins for secretion in eukaryotic cells.

The DNA fragment was inserted into unique XhoI and BglII restriction sites. Integrity of subcloned DNA sequences was confirmed using double-strand sequencing performed at Sequiserve GmbH (Vaterstetten, Germany). The fusion proteins were expressed by transient transfection of HEK293-F cells using the FreeStyle™ 293 Expression System according to the manufacturer's instruction (Invitrogen) as described above.

The huALK1-Fc-fusion and huENG-Fc-fusion molecule-containing culture supernatants were filtered and purified by two chromatographic steps. The fusion proteins were captured by affinity chromatography using HiTrap MabSelectSuRe (GE Healthcare) equilibrated with PBS (1 mM KH_2PO_4, 10 mM Na_2HPO_4, 137 mM NaCl, 2.7 mM KCl), pH 7.4. Unbound proteins were removed by washing with equilibration buffer, and the fusion protein was recovered with 0.05 M citrate buffer, pH 2.8, and immediately after elution neutralized to pH 6.0 with 1 M Tris-base, pH 9.0. Size exclusion chromatography on Superdex 200TM (GE Healthcare) was used as second purification step. The size exclusion chromatography was performed in 20 mM histidine buffer, 0.14 M NaCl, pH 6.0. Fractions containing monomeric huALK1-Fc or huENG-Fc-fusions were pooled and concentrated with an Ultrafree-CL centrifugal filter unit equipped with a Biomax-SK membrane (Millipore, Billerica, MA) and stored at −80 °C.

Biotinylation of Recombinant Human ALK1-Fc—The Avi tag containing huALK1-Fc-fusion were enzymatically biotinylated using the BirA biotin-protein ligase standard reaction kit (Avidity, LLC, Colorado) following the manufacturer's instructions. After the biotinylation, size exclusion chromatography on Superdex 200TM (GE Healthcare) was used as the purification and desalting step and performed as described above. The protein concentration of the fusion protein was determined by measuring the optical density at 280 nm using the molar extinction coefficient calculated on the basis of the amino acid sequence. Purity and integrity of the huALK1-Fc molecules were analyzed by capillary electrophoresis-SDS using a LabChip GX II (PerkinElmer Life Sciences) with Protein Express Chip and HT Protein Express Reagents kit. Aggregate content of huALK1-Fc preparations was determined by high performance size exclusion chromatography (SEC) using a TSK-GEL QC-PAK GFC 300 using 2× PBS, pH 7.4, as the running buffer or by high performance SEC using a Biosuite high resolution size exclusion chromatograph, 250 Å, 5-μm analytical size-exclusion column (Waters GmbH) using 200 mM K_2HPO_4/KH_2PO_4, 250 mM KCl, pH 7.0, as the running buffer. The percentage of biotinylation of huALK1-Fc preparations was estimated by the ability of streptavidin binding. Degree of streptavidin binding (*i.e.* biotinylation) was monitored by adding an excess of streptavidin to a sample of huALK1-Fc and performing a high performance size exclusion chromatography as described above. The integrity of the amino acid backbone of reduced Fc fusion polypeptide was verified by nanoelectrospray quadrupole TOF mass spectrometry after removal of *N*-glycans by enzymatic treatment with a combination of neuraminidase, *O*-glycanase, and peptide-*N*-glycosidase F (Roche Applied Science).

Immunoblotting—Low passage human umbilical vascular endothelial cells (Promocell) were routinely cultured in enriched endothelial cell growth medium (PromoCell) containing endothelial cell medium supplement (PromoCell) and 10% fetal bovine serum (FBS). Human umbilical vascular endothelial cells were grown to 80% confluence and serum-restricted in 0.1% FBS for 16 h. Treatment was accomplished with increasing concentrations of recombinant human mature BMP9,BMP9·pro-domain complex, and precursor BMP9 for 45 min. Cell lysates were separated on a 10% SDS-PAGE gel, and proteins were transferred to polyvinylidene fluoride membranes by semi-dry blotting. Blots were then blocked and probed with specific antibodies to Smad1 (1:1000; Cell Signaling), pSmad1/5/8 (1:1000; Cell Signaling), and Id1 (1:1000; Santa Cruz) overnight at 4 °C. Anti-human β-actin antibody (1:1000; Cell Signaling) served as the loading control. The appropriate horseradish-conjugated secondary antibody (1:2000; Cell Signaling) was added and incubated for 1 h at room temperature. Bands were visualized by chemiluminescence.

HEK293-ALK1 and Wild Type Cellular Assay—The coding sequence of human ALK1 was cloned into the pCDNA3.1 vector and transfected into HEK293 cells using X-tremeGENE9 reagent (Roche Applied Science). 1 μg of DNA was used for transfection of 10^6 cells. After 24 h, selection medium containing G418 (500 μg/ml, Roche Applied Science) was added. After 2 weeks, stabile HEK293-ALK1 clones were isolated by single cell sorting FACS (Aria II, BD Biosciences) using CF488-labeled anti-ALK1 antibody (RO68588077). Before treatment with BMP9 variants, HEK293-ALK1 and WT cells were grown to 80% confluence in MEM and subsequently serum-restricted in 0.1% FBS for 16 h. Treatment was accomplished with 2 nM recombinant human mature BMP9, BMP9·pro-domain, and precursor BMP9 for up to 24 h. Cell supernatants were subjected to ELISA measurements described below.

Confocal Microscopy—Mature BMP9 and BMP9·pro-domain were Cy5-labeled by lysine linker chemistry (protein to fluorophore ratio 1:3) and tested for binding and internalization by confocal microscopy (Eclipse TE2000E, Nikon). HEK293 and HEK293-ALK1 cells were seeded at a concentration of 3×10^3 cells/ml into μ-slides (ibidi). After 24 h, 2.5 μg/ml BMP9-Cy5 was added to the cells with or without 5 μg/ml anti-ALK1 antibody (RO68588077). Images were acquired after 24 h of incubation (excitation 638 nm; 660–700-nm emission filter).

SPR—All experiments were performed on Biacore B3000, T100, and T200 instruments (GE Healthcare) in running buffer (PBS-Tween® 20, 0.05%). Samples were diluted in running buffer supplemented with 1–2 mg/ml BSA. For analysis of the interaction of BMP9 variants with its receptors, running buffer was supplemented with 2.0 mg/ml BSA. When capture kits were used, the chip surfaces were regenerated as recommended by the vendor. Standard amine coupling was carried out as recommended by the supplier (GE Healthcare) in HBS-N buffer. Fc-tagged receptors were captured via Human-Capture kit (GE Healthcare). A series with concentrations of the interaction partner, diluted by a factor of 3, was injected with an association phase of 180 s followed by a dissociation phase of 600–3600 s depending on the dissociation rate (k_d) at a flow rate 100 μl/min. All experiments were run in duplicate or triplicate on a CM5 sensor chip at 37 °C unless stated otherwise. Capture lev-

els were adjusted to achieve a maximal analyte response R_{max} of 30 RU. Monoclonal antibody BMP9-0087 was captured via anti-rabbit-Fc (JIR) and analyzed with an association phase of 360 s followed by a dissociation phase of 3600 at a flow rate 50 μl/min. For sandwich complex formation assays, huALK1-Fc was captured via anti-human-Fc, and antibody AF3879 was amine-coupled. BMP9 variants and detection antibodies MAB3209 and AF3879 were injected consecutively using a dual inject. The contact time of each injection was 180 s, the dissociation after the second injection was monitored for 300 s. The experiment was performed with a flow rate of 30 μl/min at 25 °C. Each sample combination was analyzed as duplicate. Anti-IGF1R-Ab (RO4858696) served as a negative control. Regeneration was performed with 10 mM glycine, pH 1.5–2.5, for 60–120 s. For ternary complex formation of two receptors and BMP9, monobiotinylated human ALK1-Fc was captured via Biotin-Capture-kit (GE Healthcare). BMP9 variants, type II receptors, and ENG were injected consecutively using a dual inject. The contact time of each injection was 180 s; the dissociation after the second injection was monitored for 300 s.

Data were evaluated with BIAevaluation Software 4.1 (GE Healthcare) or Scrubber 2.0c. Binding signals were double-referenced against blank buffer and a flow cell containing no or inactive control protein. Kinetic constants were calculated from fitting to a 1:1 Langmuir binding model (refractive index = 0) unless stated otherwise. Listed K_D values represent apparent affinity values, *i.e.* avidity values, due to potential bivalent binding of dimeric BMP9 to antibodies or receptors unless stated otherwise. The ratio R_{max} is defined as R_{max} experimental/R_{max} theoretical, where 100% theoretical response maximum is calculated from the capture level of the first interaction partner (as the response units are directly proportional to molecular weight) assuming two binding sites for each dimeric mature BMP9.

BMP9 ELISA—ELISA assays "mature BMP9 ELISA," "precursor BMP9 ELISA," and "pro-domain ELISA" were developed to specifically measure the protein levels of all different BMP9 variants. A 96-well microtiter plate (MaxiSorp, Nunc) was coated with 0.5 μg/ml capture antibody MAB3209 for the mature BMP9 ELISA or the capture antibody AF3879 for the precursor BMP9 ELISA or pro-domain ELISA and incubated overnight at 4 °C on a shaker set at 450 rpm. After washing the plate 3 times with wash buffer (PBS-Tween® 20, 0.05%) it was blocked with 2% BSA in 0.1% PBS-Tween® 20 for a minimum of 60 min at room temperature. 8-Point standard curves using 2-fold serial dilutions were prepared. After a blocking and washing step, standards and pre-diluted samples were incubated for 2 h at room temperature. Incubation steps were performed on a shaker set at 450 rpm. After an additional washing step, 0.4 μg/ml concentrations of the detection antibodies BAF3209 (mature BMP9 ELISA), MAB3209 (precursor BMP9 ELISA), or BAF3879 (pro-domain ELISA) were added and incubated for 2 h at room temperature. After washing, streptavidin-horseradish peroxidase (dilution 1:10,000, Roche Applied Science) for the mature BMP9 ELISA and pro-domain ELISA or anti-mouse HRP antibody (dilution 1:8,000, Millipore) for the precursor BMP9 ELISA were incubated protected from light for 60 min at room temperature. After the final washing step, the enzymatic reaction was started with the addition of substrate solution (BM Blue POD Substrate, Roche Applied Science) followed by incubation for 20 min at room temperature protected from light. The reaction was stopped by adding stop solution (2 M H_2SO_4). With a microplate reader (VersaMax, Molecular Devices) extinction was read at a wavelength of 450 nm with a correction set at 650 nm. For the standard curve a 4PL curve fit was used. To quantify the amount of pro-domains present in the sample, the result of the precursor BMP9 ELISA and the pro-domain ELISA were subtracted.

TABLE 1
Molecular weight of BMP9 variants and fragments

BMP9 is synthesized as a precursor protein (*precursor BMP9*) that is proteolytically processed by convertases (serine endoproteases). Two active forms are described: the short mature form (*mature BMP9*) and the complexed form (*BMP9·pro-domain*) in which the pro-domains remain non-covalently associated with the mature domain. Differences in kDa values between precursor BMP9 and BMP9·pro-domain are due to amino acid exchange during construct generation (see "Experimental Procedures").

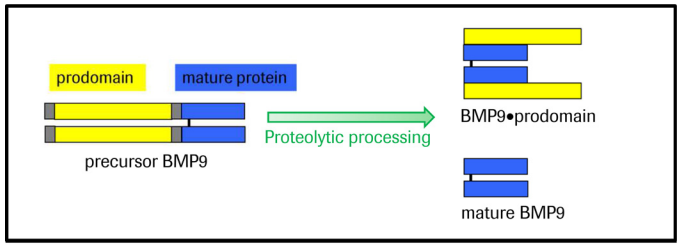

		length	kDa
precursor BMP9		aa 1 - 429	89.6
BMP9•pro-domain		aa 1 - 429	90.2
mature BMP9		aa 320 - 429	24.2
pro-domain		aa 23 - 319	66.1

Results

Bioactivity of Mature BMP, BMP9·Pro-domain, and Precursor BMP9—Both BMP9 and BMP9 in complex with its pro-domains are equally active in signaling, whereas the pro-region alone is described to be inactive (21). To obtain more information about the role of the pro-domains, mature BMP9 dimer without pro-domains, BMP9·pro-domain [2 + 2] complex with the non-covalently attached pro-domains, and full-length BMP9 precursor protein were recombinantly produced (Table 1). Generation of the precursor BMP9 protein was achieved by replacing both Arg-317 and Lys-318 by Ala to inhibit proteolytic cleavage by pro-protein convertases.

First, we tested bioactivity of equal molar amounts of all three constructs. We treated human umbilical vascular endothelial cells with increasing concentrations of mature BMP9, BMP9·pro-domain complex, and precursor BMP9. Although mature BMP9 growth factor and BMP9·pro-domain induced Smad protein 1, 5- and 8 phosphorylation and Id1 expression, precursor BMP9 was inactive (Fig. 1).

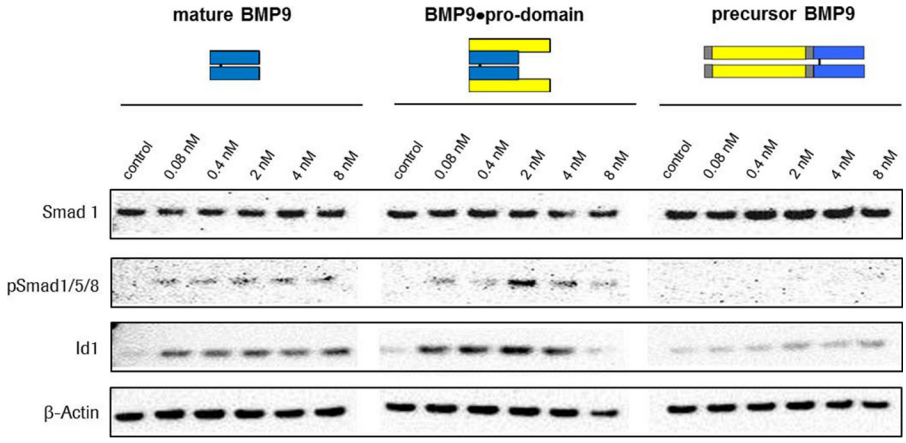

FIGURE 1. **Biological activity of recombinant BMP9 variants.** Biological activity of increasing concentrations of mature BMP9, BMP9·pro-domain, and precursor BMP9 determined by the ability to induce Smad protein 1, 5, and 8 phosphorylation and Id1 expression.

BMP9·Pro-domain Binding to ALK1, Type II Receptors, ENG, or Anti-mature BMP9 Antibodies Led to Complete Displacement of Pro-domains—To investigate binding kinetics of the different BMP9 variants, Biacore experiments were performed using the ECD of ALK1 linked to a Fc domain of human IgG (ALK1-Fc). After immobilization of the chimeric ALK1-Fc protein on a CM5 chip, mature BMP9, BMP9·pro-domain, and precursor BMP9 were injected at various concentrations, and binding was recorded. In accordance with published results (13, 24), mature BMP9 bound to ALK1 with high avidity and an apparent K_D in the low pM range with a fast association rate ($k_a = 6.3 \times 10^6$ M^{-1}s^{-1}) and a slow dissociation rate ($k_d \leq 5.0 \times 10^{-5}$ s^{-1}) (Fig. 2*A* and Table 2). When BMP9·pro-domain was tested as an analyte, a similar sensorgram and a comparable K_D were obtained (Fig. 2*A* and Table 2), indicating that the pro-domain moiety does not seem to interfere with binding of the mature part to ALK1. Using precursor BMP9 under identical assay conditions, a significantly decreased association rate constant k_a by factor ~250 was observed (Fig. 2*A* and Table 2). The resulting avidity differed by the same order of magnitude, arguing for a steric hindrance caused by the pro-domains.

The BIAevaluation software allowed analysis of BMP9 binding capacity (called R_{max}, for maximum response), which in this assay setup theoretically corresponds to saturation of all ALK1-Fc chimeric receptor molecules by the ligand. The experimentally obtained R_{max} value can be set in relation to the expected saturation signal and expressed as ratio R_{max} in percentage. This ratio R_{max} for ALK1-Fc interaction with mature BMP9 was determined to be 69% (Table 2). This is reasonable, as 100% is rarely achieved in reality, and slightly lower values can be explained by partially misfolded components in the recombinant chimeric receptor preparation. The ratio R_{max} for the interaction with BMP9·pro-domain surprisingly was only 19% (Table 2). There is no reasonable explanation for such a dramatic change as in both runs the same batch of ALK1-Fc was used. Because SPR signals are directly proportional to the molecular weight, the immediate assumption was that not the entire molecule of pro-domain-complexed BMP9 is part of the formed receptor-ligand complex. Assuming that only mature BMP9 is part of the complex, despite providing BMP9·pro-domain for binding to ALK1-Fc, the re-calculated ratio R_{max} changed to 69%, in good accordance with the complex formation with mature BMP9 (Table 2).

Because BMP9 signaling via ALK1 is modulated by type II co-receptors and ENG, we were interested whether BMP9·pro-domain might have a preference for certain co-receptors or whether pre-binding to ALK1 with displacement of the pro-domain is even a prerequisite for subsequent co-receptor recruitment. To this end, we measured kinetic interactions of mature BMP9 or BMP9·pro-domain with BMPRII, ActRIIA, ActRIIB, and ENG ECDs linked to the Fc domain. Kinetic constants obtained for mature BMP9 were in good accordance with published data (13, 25), except for ENG-Fc, which showed fast on-off kinetics in our hands with an apparent affinity of 2.7 nM (quality differences in ENG preparations and in particular in the experimental set-up might account for this deviation; *e.g.* Castonguay *et al.* (25) reported mass transport limitations in their Biacore runs) (Figs. 2*B* and 3, *A–C*, and Table 2). Precursor BMP9 was not significantly bound by any of the co-receptors (data only shown for BMPRII; Fig. 2*B* and Table 2). Importantly, practically identical values were measured with both mature BMP9 and BMP9·pro-domain for all receptors (Figs. 2 and 3 and Table 2), and maximal responses R_{max} again indicated that the pro-domain must have been released from the complex (Table 2).

Interestingly, an analogous mechanism was found for anti-BMP9 antibodies recognizing mature BMP9. When antibody BMP9-0087 captured via Fc was exposed to mature BMP9 or BMP9·pro-domain, comparable kinetic profiles and constants were observed (Fig. 3*D* and Table 2). The pro-domain release and its kinetics were even conserved between species, as shown with the corresponding recombinant human, mouse, and cynomolgus macaque proteins (data not shown).

Further Evidence of Pro-domain Displacement Provided by Sandwich Complex Formation Biacore Assays—Next, we performed sandwich complex formation Biacore experiments with ALK1-Fc captured via Fc part exposed to either mature BMP9, BMP9·pro-domain, precursor BMP9, or pro-domains. Immediately after the association of the ligand, detection antibodies recognizing either mature BMP9 (MAB3209) or the pro-do-

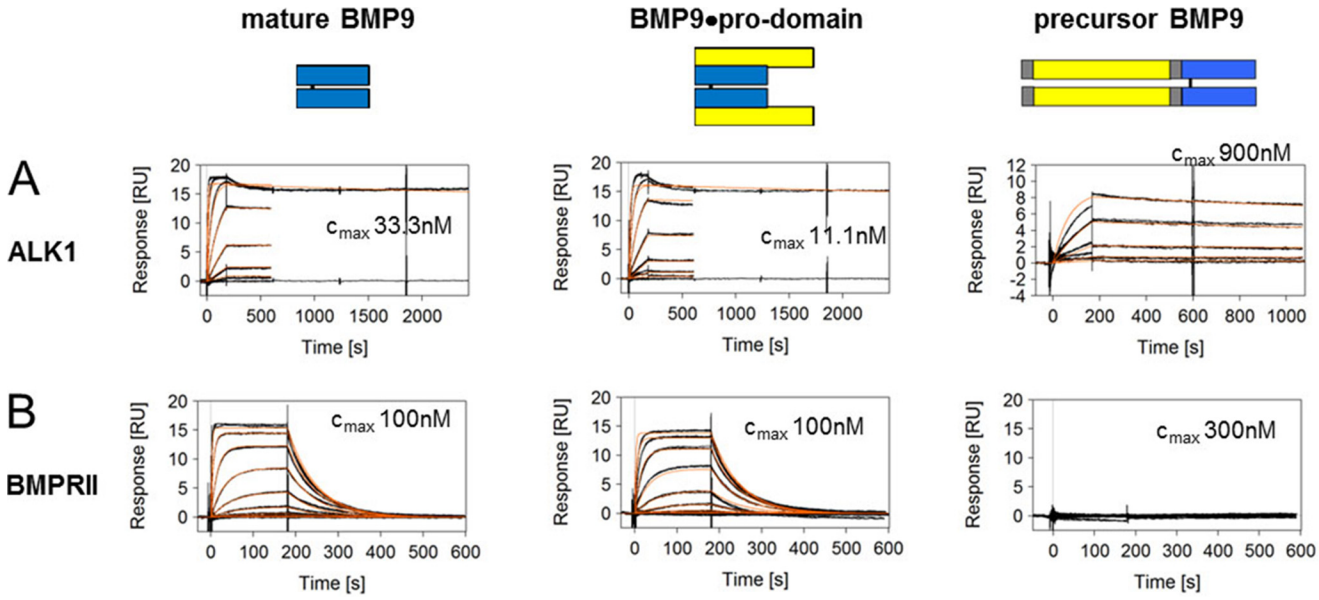

FIGURE 2. **Binding profile of BMP9 variants to ALK1 and BMPRII.** SPR sensorgrams of mature BMP9, BMP9·pro-domain, and precursor BMP9 binding to ALK1 (*A*) and BMPRII (*B*). Measured biomolecular interactions were evaluated using a regular 1:1 Langmuir binding model. Different concentrations are shown in *black* with maximum concentrations indicated, and the curve fittings are shown in *red*. *RU*, response units.

TABLE 2

Kinetic interaction parameters for BMP9 variants binding ALK1, type II receptors, ENG, and α-BMP9-mAb BMP9-0087 at 37 °C

Association (k_a) and dissociation (kd) rate constants, half times ($t_{1/2}$), and the resulting dissociation equilibrium constants K_D as determined by BIAevaluation Software using a 1:1 Langmuir fit are shown with the S.E. K_D values represent avidity instead of affinity due to possible bivalent binding of dimeric BMP9-ligand to the dimeric receptors. R_{max}: *, calculated for release of pro-domain; **, calculated for pro-domain as part of complex.

on chip	BMP9 variants	k_a [$M^{-1}·s^{-1}$]	k_d [s^{-1}]	$t_{1/2}$ [min]	K_D [M]	ratio R_{max} [%]*	ratio R_{max} [%]**
hu ALK1-Fc	hu mature BMP9	6.3 x 10^6 ± 0.1 %	<5.0 x 10^{-5} ± 0.3 %	<231.0	<8.0 x10^{-12}	69.3	
	hu BMP9•pro-domain	8.3 x 10^6 ± 0.1 %	<5.0 x 10^{-5} ± 0.3 %	<231.0	<6.0 x10^{-12}	68.8	18.5
	hu precursor BMP9	1.7 x 10^4 ± 0.2 %	7.0 x 10^{-5} ± 2.9 %	165.0	4.1 x10^{-9}		38.3
hu BMPRII-Fc	hu mature BMP9	4.7 x 10^6 ± 0.1 %	1.5 x 10^{-2} ± 0.03 %	0.8	3.3 x10^{-9}	75.4	
	hu BMP9•pro-domain	4.7 x 10^6 ± 0.1 %	1.5 x 10^{-2} ± 0.1%	0.8	3.2 x10^{-9}	72.1	19.3
	hu precursor BMP9	no binding detectable					
hu ActRIIA-Fc	hu mature BMP9	steady state affinity			42.7 x10^{-9} ± 0.2 %	54.7	
	hu BMP9•pro-domain	steady state affinity			19.7 x10^{-9} ± 0.4 %	29.3	7.9
	hu precursor BMP9	no binding detectable					
hu ActRIIB-Fc	hu mature BMP9	3.9 x 10^6 ± 0.2 %	5.6 x 10^{-3} ± 0.1 %	2.1	1.4 x10^{-9}	4.8	
	hu BMP9•pro-domain	5.5 x 10^6 ± 0.1 %	4.3 x 10^{-3} ± 0.1 %	2.7	0.8 x10^{-9}	3.6	1.0
	hu precursor BMP9	no binding detectable					
hu ENG-Fc	hu mature BMP9	steady state affinity			2.7 x10^{-9} ± 0.4 %	82.5	
	hu BMP9•pro-domain	steady state affinity			1.5 x10^{-9} ± 0.7 %	67.9	18.2
	hu precursor BMP9	very weak binding detectable					
α-BMP9-Mab	hu mature BMP9	1.0 x 10^7 ± 1.0 %	<5.0 x 10^{-5} ± 1.0 %	>231.0	<5.0 x 10^{-12}	84.0	
	hu BMP9•pro-domain	1.4 x 10^7 ± 0.3 %	<5.0 x 10^{-5} ± 0.2 %	>231.0	<3.6 x 10^{-12}	80.2	21.5

main (AF3879) were administered in a subsequent injection leading to a ternary complex in case of successful binding (Fig. 4*A*). As expected, anti-BMP9 antibody MAB3209 detected mature BMP9 in complex with ALK1, whereas anti-pro-domain antibody AF3879 showed no signal, similar to control buffer (Fig. 4*B*). Interestingly, after complex formation of the receptor with BMP9·pro-domain on the chip surface, the pro-domain was no longer detectable by AF3879, suggesting that the pro-domain is displaced upon receptor binding (Fig. 4*C*). In contrast, precursor BMP9 in complex with ALK1 was recognized by both anti-mature BMP9 antibody MAB3209 and anti-pro-domain antibody AF3879 (Fig. 4*D*). The isolated pro-domain did not bind to

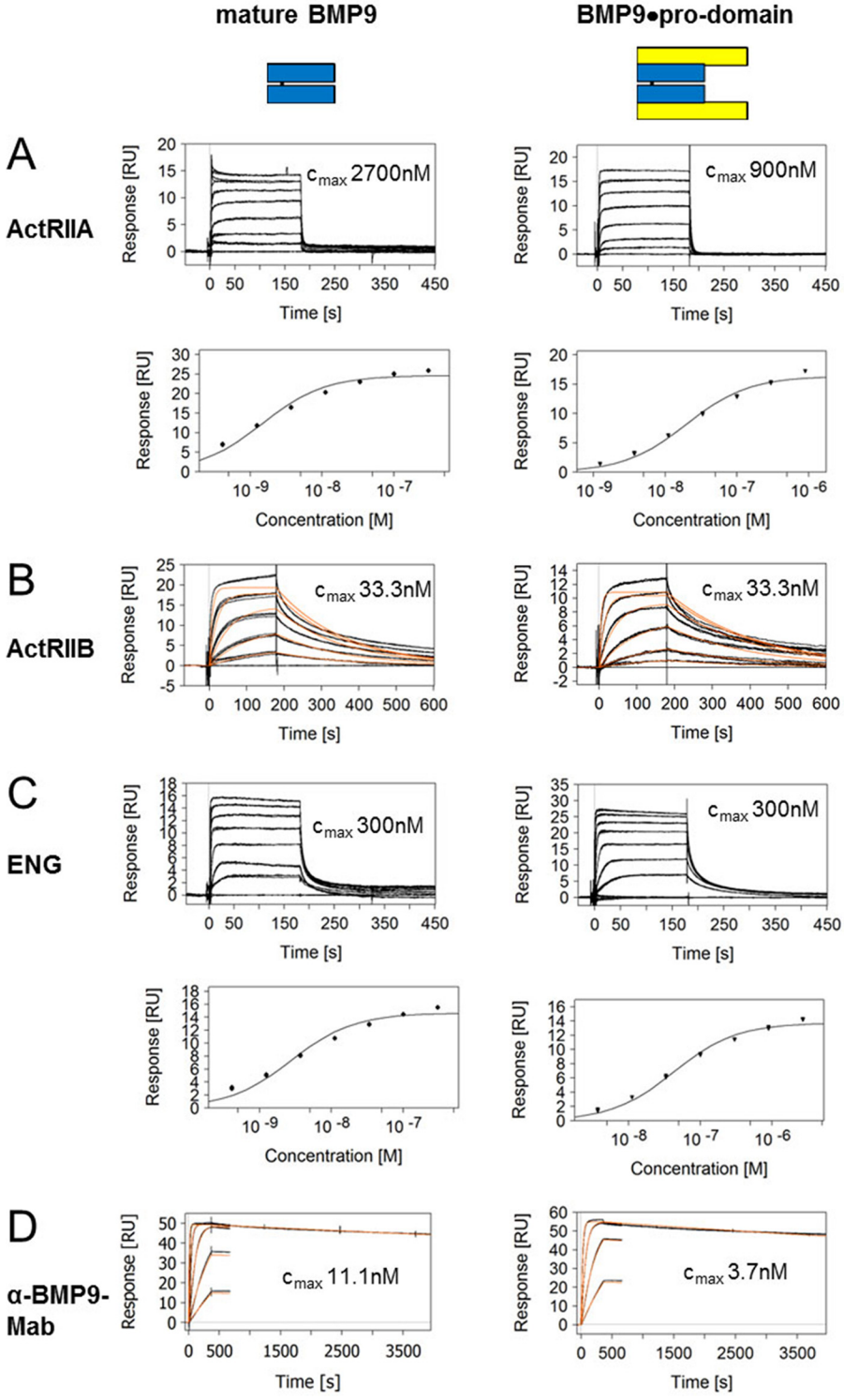

FIGURE 3. **Binding profile of mature BMP9 and BMP9·pro-domain to ActRIIA, ActRIIB, ENG, and anti-mature BMP9 antibody.** SPR sensorgrams of BMP9 binding to ActRIIA (*A*), ActRIIB (*B*), ENG (*C*), and anti-mature BMP9 (*D*) antibody BMP9-0087. Measured biomolecular interactions were evaluated using a regular 1:1 Langmuir binding model for *B* and *D*. Different concentrations are shown in *black* with maximum concentrations indicated, and the curve fittings are shown in *red*. For the fast interactions in *A* and *C* affinities were evaluated in an equilibrium steady state model from responses at the 150–160-s time window, with fitting depicted *below the corresponding sensorgrams*. *RU*, response units.

ALK1 (Fig. 4*E*). Sandwich complex formation experiments using immobilized anti-mature BMP9 antibodies also demonstrated similar results to those obtained with ALK1-Fc (data not shown).

Furthermore, we analyzed whether ternary complexes of type II receptors BMPRII, ActRIIA, and ActRIIB and co-receptor ENG could be formed with ALK1 that had been pre-complexed with BMP9 variants on a Biacore chip (Fig. 5*A*). Indeed, ternary complexes of type II receptors BMPRII, ActRIIA, and ActRIIB and co-receptor ENG formed with ALK1 regardless of whether mature BMP9 or BMP9·pro-domain was applied, once

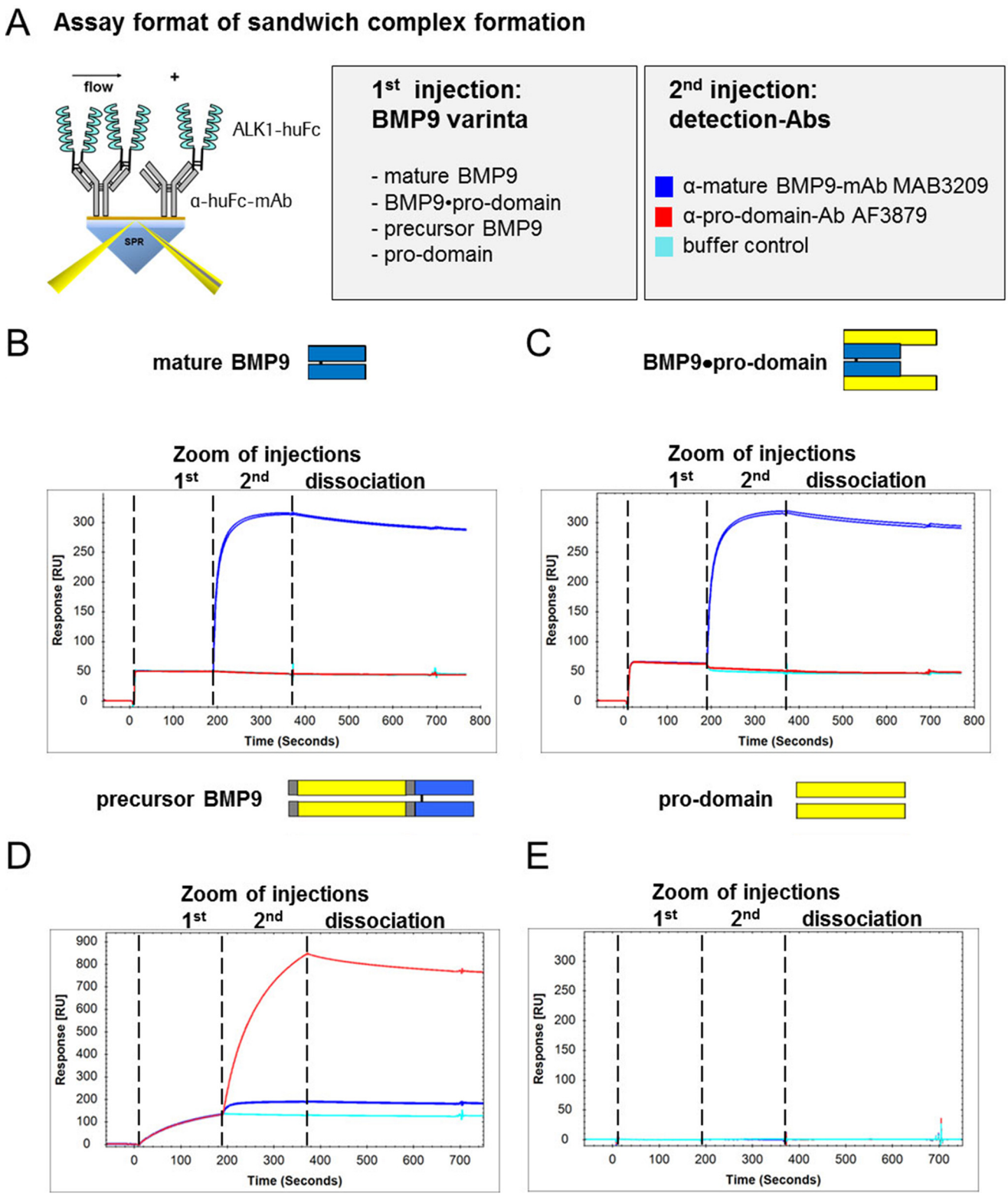

FIGURE 4. **Deciphering the mode of action of pro-domain displacement, investigated by Biacore sandwich complex formation assays.** To further dissect the interaction of BMP9 variants with ALK1, sandwich complex formation SPR assays were designed. The illustration in *A* visualizes the assay setup. ALK1-Fc was captured via Fc part on a CM5-Chip. BMP9 variants and detection antibodies α-mature BMP9-mAb MAB3209 or α-pro-domain-Ab AF3879 were injected consecutively using a dual inject. Sensorgrams for complex formations are shown for mature BMP9 (*B*), BMP9·pro-domain (*C*), precursor BMP9 (*D*), and pro-domain (*E*) as the first analyte injected. After complex formation of the receptor with BMP9 variants on the chip surface, the pro-domain was only detected for the precursor BMP9 by pro-domain-specific antibody AF3879 in a subsequent injection (*D*).

more corroborating our findings of pro-domain release (Fig. 5, *B* and *C*). Ternary complex formation was furthermore independent from the order of binding events; co-receptor or type II receptors could also be preincubated with BMP9 variants in solution and offered to soluble ALK1-Fc on the chip with identical results obtained (data not shown).

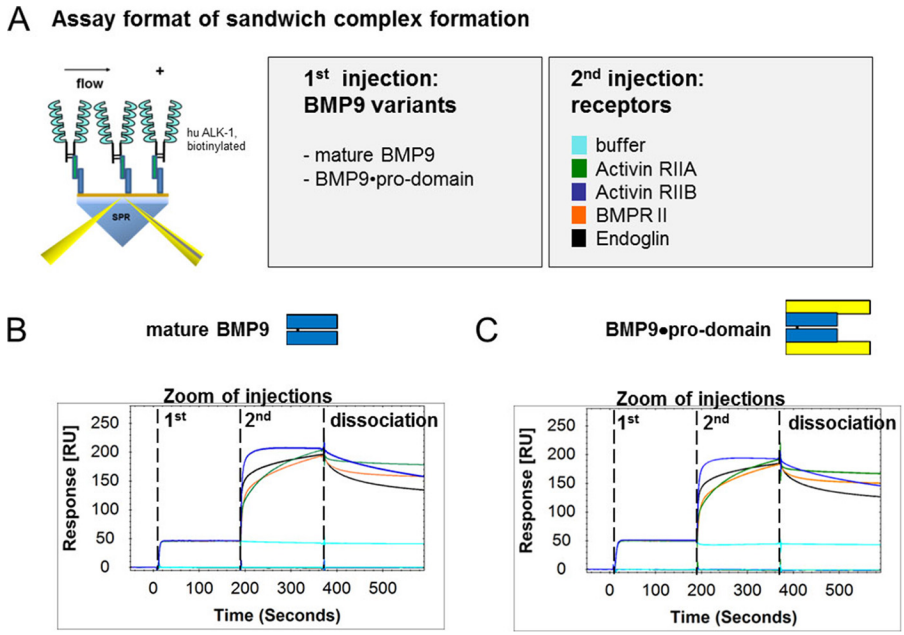

FIGURE 5. **Ternary complex formation of BMP9 variants and ALK1, type II receptors, or ENG.** To analyze if ternary complexes of type II receptors BMPRII, ActRIIA, and ActRIIB and co-receptor ENG could form with ALK1 pre-complexed with BMP9, the assay setup visualized in *A* was applied. Biotinylated ALK1 was captured on a Biacore chip. Mature BMP9 variants and receptors were injected consecutively using a dual inject. Sensorgrams for complex formations are shown for mature BMP9 (*B*), and BMP9·pro-domain (*C*) with the respective receptors. *RU*, response units.

Release of the Pro-domains Was a Rapid Process—To get further insight into the mechanism of pro-domain displacement, we analyzed by Biacore whether the association time of BMP9·pro-domain to ALK1 would influence complex stability (Fig. 6). If after an initial fast contact a slower second step or a large conformational rearrangement was rate-limiting, one would expect a more stable complex after a longer association time. We observed identical dissociation rates after 60- and 360-s associations (Fig. 6), indicating that there is no such complex mechanism or that it is at least a very fast process. Similar results were obtained using anti-BMP9 antibody (data not shown).

BMP9·Pro-domain Binding to Anti-pro-domain Antibody Led to Release of Mature BMP9 Growth Factor—For subsequent ELISA assays it was relevant to know whether antibody binding to the pro-domain would likewise release the mature BMP9 from the BMP9·prodomain complex. Therefore, we performed sandwich complex formation Biacore experiments with anti-pro-domain antibody AF3879 and BMP9 variants analogous to the ones described above. Immediately after the association of the ligand, detection antibodies recognizing either mature BMP9 (MAB3209) or the pro-domain (AF3879) were administered in a subsequent injection leading to a ternary complex in case of successful binding (Fig. 7*A*). As expected, no binding was detected with mature BMP9 (Fig. 7*B*). After complex formation of anti-pro-domain antibody AF3879 with BMP9·pro-domain on the chip surface, the pro-domain was detectable by AF3879 (because the polyclonal antibody recognizes several non-overlapping epitopes), but surprisingly the mature growth factor domain was no longer recognized by anti-BMP9 domain antibody MAB3209 (Fig. 7*C*). This argues for a release of the mature BMP9 growth factor from pro-domain complexed BMP9. As expected, precursor BMP9 in complex with anti-pro-domain antibody AF3879 was recognized by both antibodies specific for either mature BMP9 (MAB3209) or the pro-domain (AF3879) (Fig. 7*D*). Also, the isolated pro-domains showed binding only to the respective antibodies (Fig. 7*E*).

Biochemical Characterization of BMP9 Variants by ELISA—The Biacore experiments that revealed displacement of pro-domains and mature growth factor from BMP9·pro-domain complex were corroborated by ELISA studies. For these experiments, different capture antibodies were absorbed on the well surface of microtiter plates, and combinations of different detection antibodies were used to quantify the protein levels of all different BMP9 variants. Although mature and precursor BMP9 were directly detectable by ELISA, BMP9·pro-domain complex could only be measured indirectly as dissociated fragments due to displacement of mature growth factor and pro-domains after antibody binding (Fig. 8*A*). As a consequence, three different ELISAs were developed: (i) mature BMP9 ELISA for detection of free mature BMP9 as well as the mature BMP9 from dissociated BMP9·pro-domain variant (Fig. 8*B*); (ii) precursor BMP9 ELISA for detection of precursor BMP9 protein (Fig. 8*C*); (iii) pro-domain ELISA for detection of pro-domains as part of the BMP9·pro-domain variant (Fig. 8*D*). Additionally, this assay detects also precursor BMP9 (Fig. 8*D*).

ELISA-based calculations also prove that in each case only a proportion (either mature domain or pro-domain) of the BMP9·pro-domain complex can be measured and that pro-domains or mature growth factor are separated from the complex after antibody binding. When BMP9·pro-domain complex standard was applied with a maximum concentration of 250 pg/ml, a total value of 67 pg/ml was detectable using the mature BMP9 ELISA (mature BMP9 24.2 kDa/BMP9·pro-domain 90.2 kDa × 250 pg/ml = 67 pg/ml; Fig. 8*B*; see Table 1 for comparison of molecular masses). When BMP9·pro-domain complex stan-

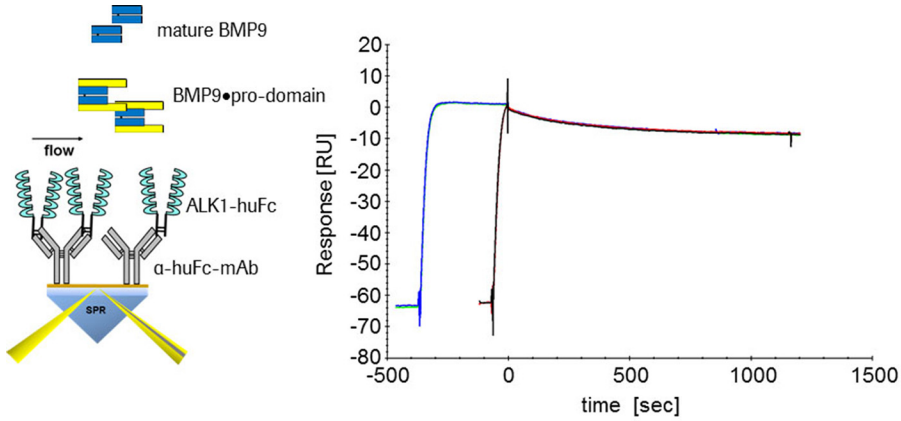

FIGURE 6. **Variable association of BMP9·pro-domain binding to ALK1.** ALK1-Fc was captured via Fc part on a CM5-Chip and BMP9·pro-domain was offered as an analyte. Identical dissociation rates were observed after 60 and 360 s association. *RU*, response units.

dard was applied with a maximum concentration of 1000 pg/ml, a total value of 732 pg/ml was detectable using the pro-domain ELISA (pro-domain 66.1 kDa/BMP9·pro-domain 90.2 kDa × 1000 pg/m = 733 pg/ml; Fig. 8*D* and Table 1). ELISA experiments also confirmed release of mature BMP9 growth factor after anti-pro-domain antibody binding. The mature BMP9 ELISA detected dissociated mature BMP9 domain in the ELISA supernatant of the pro-domain ELISA after BMP9·pro-domain binding (Fig. 9, *A* and *B*).

Using our novel ELISAs we sought to specify the proportion of the different BMP9 variants in human plasma. To quantify the amount of pro-domains present in the sample, the result of the precursor BMP9 ELISA and the pro-domain ELISA were subtracted. As a result of antibody-mediated pro-domain and mature growth factor displacement, BMP9·pro-domain complex was measured indirectly with a double signal both in the mature growth factor (0.5%) and pro-domain fractions (77.5%), whereas precursor BMP9 (22%) was detected directly (Fig. 10*A*). Hence, free mature BMP9 and the mature BMP9 domain of the dissociated BMP9·pro-domain variant cannot be discriminated. If we neglect the proportion of free mature BMP9 for convenience reasons, we can estimate that the majority of BMP9 (77%) in the biological samples are pro-domains. Interestingly, although pro-domains and precursor BMP9 could also be measured in serum, mature BMP9 was detectable in plasma samples only (data not shown). Comparison of the average concentration of mature BMP9 in human and mouse plasma demonstrated lower concentration levels for mature BMP9 in mouse plasma (~120 pg/ml human and ~50 pg/ml mouse mature BMP9; Fig. 10*B*). As human mature BMP9 corresponds to 0.5% of total BMP9 in human plasma (Fig. 10*A*), the total concentration of active human BMP9 can be estimated to ~444 pg/ml if free mature BMP9 is neglected (~120 pg/ml × 3.7; see Table 1 for comparison of molecular masses of BMP9 variants).

Pro-domain Release Occurred also upon Binding of BMP9·Pro-domain to Living Cells—Pro-domain displacement mediated by membrane-bound ALK1 on living cells was monitored on ALK1-transfected or wild type HEK293 cells as the negative control by our ELISA assays (Fig. 11*A*). In the supernatant of HEK293-ALK1 cells, signals for BMP9 decreased regardless of whether mature or BMP9·pro-domain was applied (Fig. 11*A*), whereas amounts of precursor BMP9 or pro-domain remained stable throughout the duration of the experiment (24 h; Fig. 11*A*). The decrease was contributed to internalization of mature or pro-domain complexed BMP9 by confocal microscopy (Fig. 11*B*). In summary, our results establish a model of complete displacement of the non-covalently bound pro-domains after binding of BMP9·pro-domain to ALK1 and type II receptors (or anti-mature BMP9 antibodies) leading to rapid activation of the signaling process (Fig. 12).

Discussion

Like BMP9, other TGFβ family members were shown to remain associated with their pro-domains after secretion, including TGFβ, BMP2, BMP4, BMP5, BMP7, BMP10, GDF5, and myostatin (GDF8) (26). The pro-domains can modulate the activities of the mature domains. Whereas TGFβ and BMP10 are latent as pro-domain-growth factor complexes, BMP4, BMP7, and BMP9 are non-covalently associated with their propeptide chains in a bioactive complex (16, 21). Receptor binding of pro-domain-complexed growth factors appears to be complex, depending on both the receptor type and the individual pro-form. Here we show that type I receptor ALK1, all relevant type II, and co-receptor ENG *per se* can readily recognize the pro-domains of BMP9·pro-domain complex, which leads to complete displacement of the pro-domain after receptor binding. Interaction of BMP9·pro-domain with ALK1 and type II receptors was recently analyzed by ELISA applying a direct coating of human BMP9 fused to a murine pro-domain (22). In accordance to our data, little effect on the affinities for ALK1 was shown, but in contrast to our findings both the EC_{50} and the selectivity of type II receptor binding was altered by pro-domain complexation (22). We use soluble BMP9 in our SPR assay setup and hereby demonstrate that all receptors investigated behave similarly to ALK1 with regard to BMP9·pro-domain binding. Complexation of circulating BMP9 by its pro-domain does not, therefore, seem to play a role in modulating signaling via one or the other hetero-tetrameric receptor complex. This observation is interesting, as it implicates no temporal and spatial signaling specificity of BMP9 and no partial inhibition of BMP9 signaling by the pro-domain, underscoring the importance of constitutively active circulating BMP9 (1). Fur-

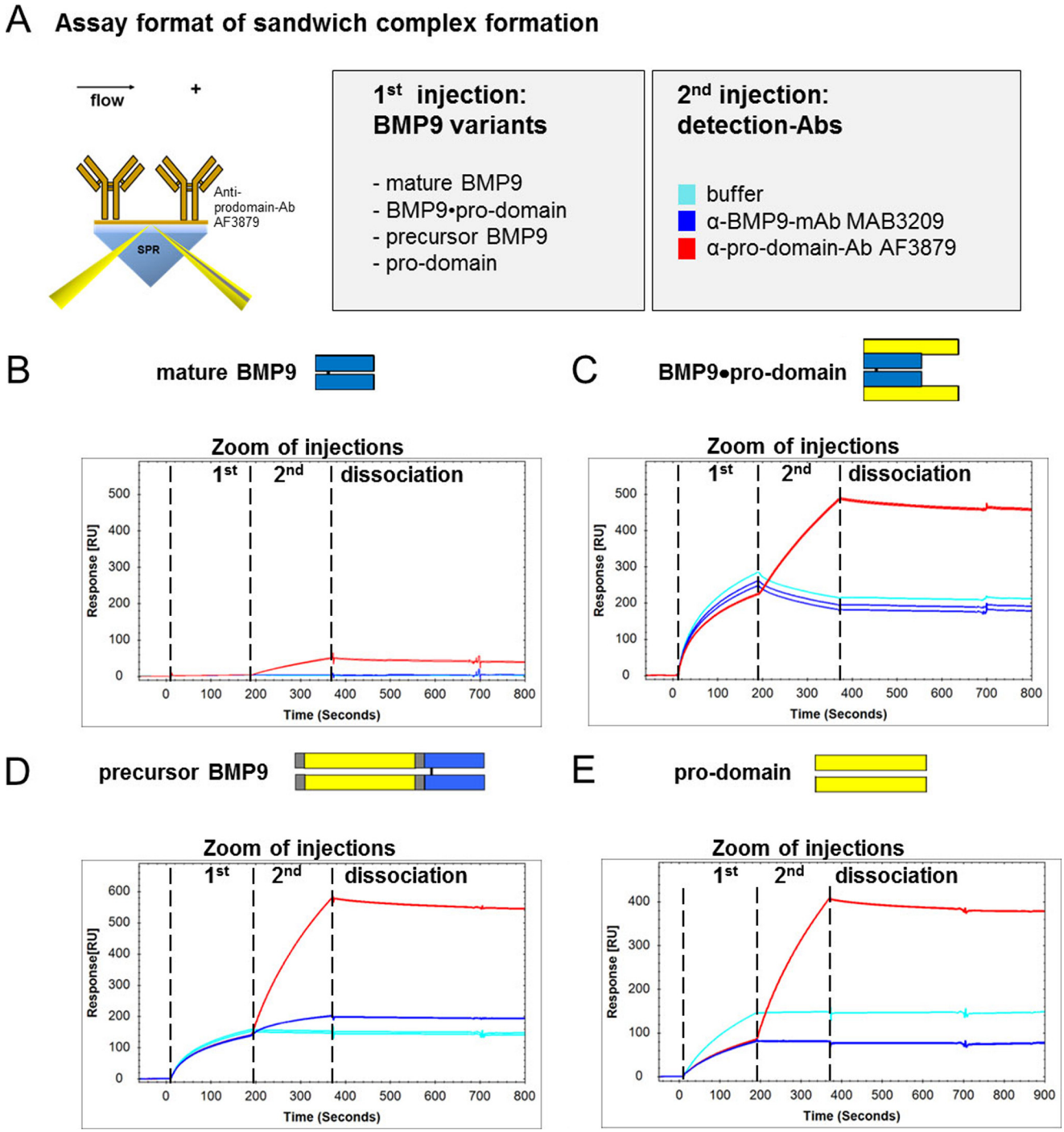

FIGURE 7. **Deciphering the mode of action of mature BMP9 growth factor release, investigated by Biacore sandwich complex formation assays.** To determine the interaction of BMP9 variants with anti-pro-domain antibody AF3870, sandwich complex formation assays were designed. The illustration in *A* visualizes the assay setup. Anti-pro-domain antibody AF3870 was amine-coupled on a CM5-Chip. BMP9 variants and detection antibodies α-mature BMP9-mAb MAB3209 or α-pro-domain-Ab AF3879 were injected consecutively using a dual inject. Sensorgrams for complex formations are shown for mature BMP9 (*B*), BMP9·pro-domain (*C*), precursor BMP9*D*), and pro-domain (*E*) as the first analyte injected. After complex formation of the antibody with BMP9 variants on the chip surface, the mature BMP9 domain was only detected for the precursor BMP9 by mature domain-specific mAb MAB3209 in a subsequent injection (*D*). *RU*, response units.

thermore, we demonstrate that the release of the pro-domains is a rapid process that ensures speedy activation and bioavailability of BMP9 and helps to explain how BMP9 can serve as a vascular quiescence factor (1).

Although an open-armed conformation similar to BMP9 was described for the bioactive BMP7·pro-domain complex (22), interestingly, in this case, type I receptors BMPRIA (ALK3) and BMPRIB (ALK6) interact with the BMP7·pro-domain complex without displacing the pro-domains. The type II receptors ActRIIA, ActRIIB, and BMPRII compete with the pro-domain for binding to the growth factor resulting in a stepwise pro-domain displacement (26). The partially latent BMP2·pro-domain complex was shown to bind to type I receptor BMPRIA but not to type II receptor BMPRII (27). The pro-domain is

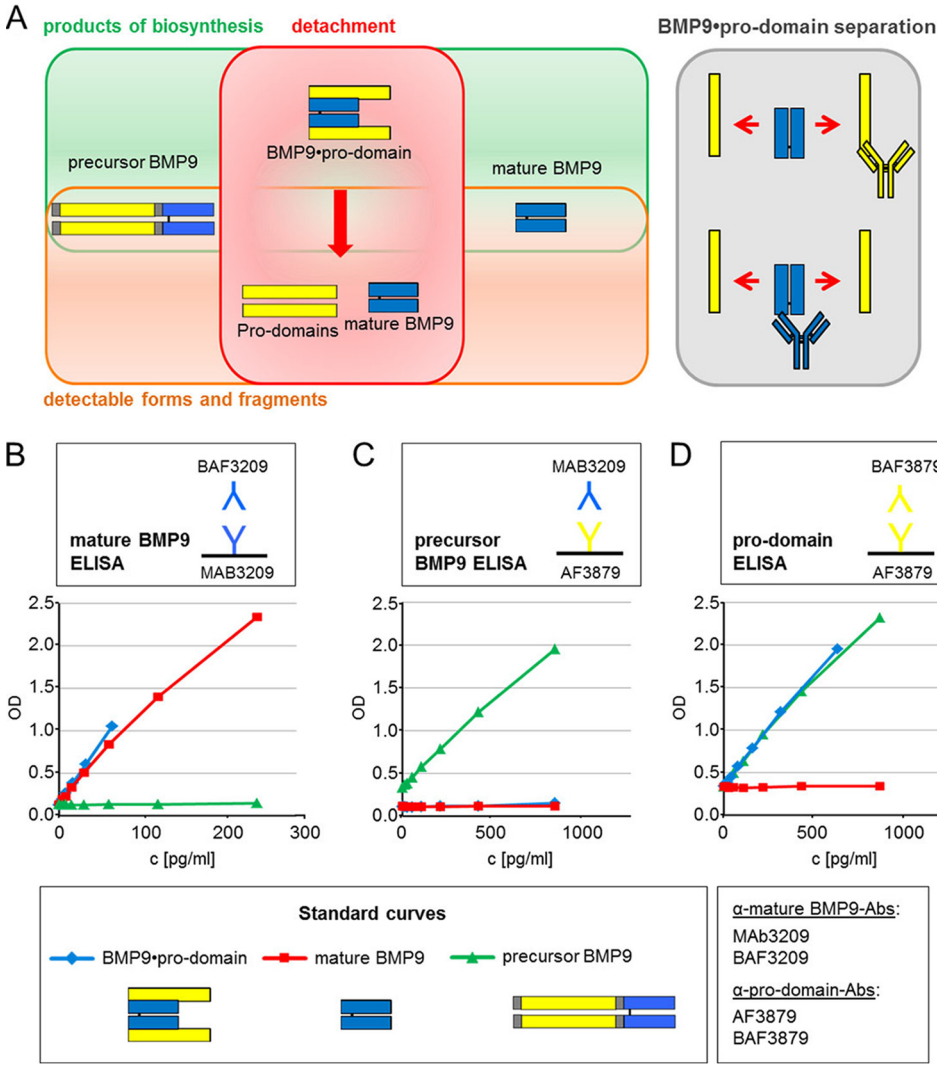

FIGURE 8. **ELISA setup for detection of different circulating BMP9 variants.** *A*, as a consequence of pro-domain displacement, BMP9·pro-domain complex is measured indirectly by ELISA as displaced mature growth factor and pro-domain fragments. *B–D*, development of different ELISAs for the detection of mature BMP9 (mature BMP9 ELISA) (*B*), precursor BMP9 protein (precursor BMP9 ELISA) (*C*), and pro-domains (*D*) as part of the fragmented BMP9·pro-domain variant (pro-domain ELISA). Additionally, the pro-domain ELISA detects precursor BMP9.

suggested to target a variety of TGFβ growth factor family members (*e.g.* TGFβ, BMP2, BMP4, BMP5, BMP7, BMP10, and GDF5) to the extracellular matrix by binding to latent TGF binding proteins or fibrillins (17, 28). The pro-domain of GDF8 interacts with the glycosaminoglycan side chain of perlecan (16). Interactions of pro-domains with the microfibril network are considered as an extracellular storage site, important for positioning and concentrating growth factors in the extracellular matrix (29). Furthermore, complex formation with latent TGF binding proteins and fibrillin microfibrils could possibly render bioactive complexes of growth factors and pro-domains latent once they are bound, as this high affinity binding also seems to strengthen the pro-domain-growth factor complex (30). As for BMP9, binding to matrix molecules has not yet been shown, but it was proposed that binding to interactors in the matrix may regulate transition between an active, signaling-competent open-armed and a proposed latent cross-armed conformation to regulate BMP9 growth factor latency (22). The ease by which BMP9 is released from its pro-domain complex by all receptors and antibodies investigated here leads us to speculate that matrix binding would not retain BMP9 in a stable complex either and would, therefore, not serve any biological role. Further studies are needed to determine the interaction of the BMP9 pro-complex with extracellular matrix components (31, 32). BMP9 and BMP10 belong to the same subgroup of the TGFβ superfamily based on amino acid sequence similarities and exhibit similar functions during early development (5, 6). The pro-domains of cardiac-specific BMP10 were proposed to confer latency to the BMP10·pro-domain complex and to regulate interactions with fibrillin-1 in the extracellular space (17). Specific activation of latent BMP10·pro-domain complexes was achieved by cleavage of the pro-domain by the metalloprotease BMP1 (16). A recent study, however, reveals that the BMP10·pro-domain is active in multiple endothelial cells and that the ECD of BMPRII can release BMP10 from the pro-domain complex (33). Questions remain of how these very similar growth factors function differently in a tissue-specific manner, as BMP10 exhibits a unique role during cardiac development that cannot be compensated by BMP9 (6).

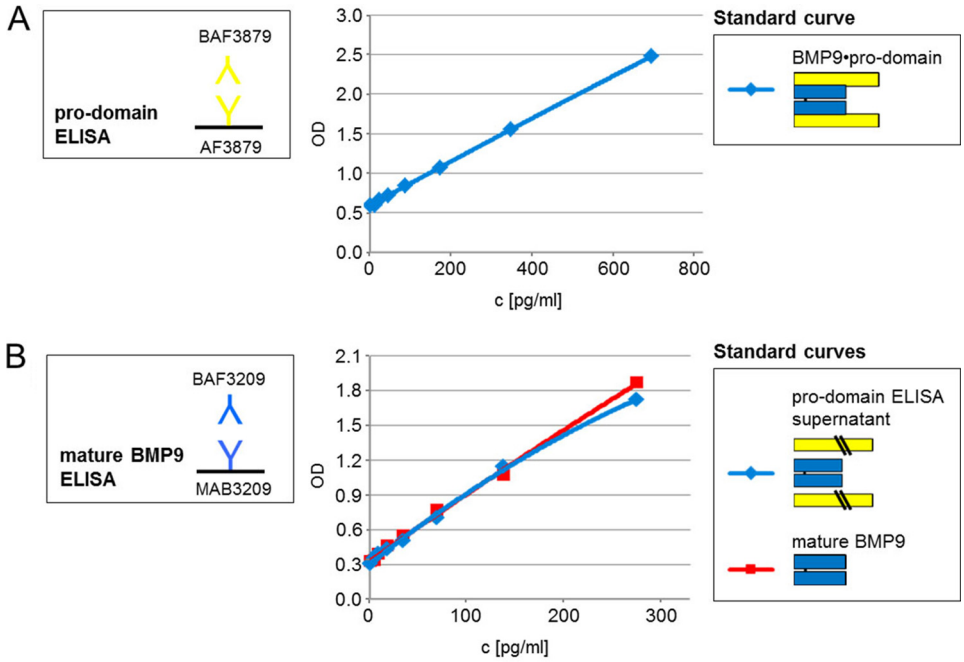

FIGURE 9. **Release of mature growth factor from BMP9·prodomain complex.** Release of mature BMP9 domain after binding of an anti-pro-domain antibody was confirmed by application of BMP9·pro-domain to the pro-domain ELISA using anti-pro-domain antibodies AF3879 as capture and BAF3879 as detection (*A*). *B*, supernatant from *A* and recombinant mature BMP9 standard were applied to the mature BMP9 ELISA using anti-mature BMP9 antibodies MAB3209 as a capture and BAF3209 as detection. The mature BMP9 ELISA detected both mature BMP9 standard and released mature BMP9 from pro-domain ELISA supernatant.

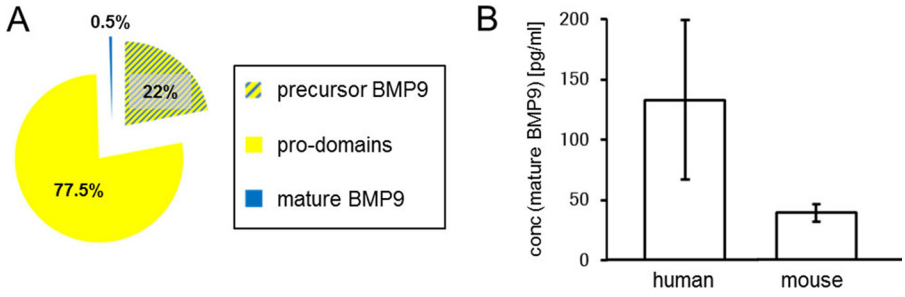

FIGURE 10. **BMP9 circulating variants in human plasma.** *A*, P_i chart representing the percentage of mature BMP9, precursor BMP9, and pro-domains circulating in human plasma. *B*, average concentration of human and mouse mature BMP9 with human BMP9 corresponding to 0.5% of total BMP9 in human plasma (*A*). The murine BMP9 pro-domains and precursor protein were not detectable in this assay setup due to lack of mouse cross-reactivity of anti-pro-domain antibody AF3879 (data not shown).

BMP9 is potent in activating ALK1, with an EC_{50} of 50 pg/ml (1). Circulating levels of BMP9 were described to be between 2 and 10 ng/ml measured by activity (1, 34). In this study concentrations of active BMP9 were found to be ~444 pg/ml in human plasma as determined by ELISA. Interestingly, mechanisms for the regulation of constitutively active circulating BMP9 were described (35). Stable BMP9 dimers were shown to form either covalently (with intermolecular disulfide bond; D-form) or non-covalently (without intermolecular disulfide bond; M-form). Both forms were capable of binding to the pro-domain and ALK1, but the M-form displayed greater susceptibility to redox-dependent cleavage by proteases present in serum (35).

BMP9 has emerged as a powerful growth factor currently at the forefront of bone healing technologies (36) and as a therapeutic target in neurodegenerative disease (37) and cancer (38). Administration of BMP9 holds therapeutic potential in bone and cartilage defects and neurodegenerative disease (36, 37). In addition, targeting BMP9/BMP10 signaling by soluble Alk1-Fc and an ALK1 blocking antibody is explored in cancer treatment (23, 38). In this study, we show that upon binding to the complex of mature part and pro-domains, BMP9 receptors or targeting antibodies are able to completely dissociate the pro-domains from the complex. In addition to the described physiological implications of our findings, the displacement of the pro-domains is of significant translational interest for ELISA measurement of BMP9 circulating variants, a method that may be important for present and future research regarding BMP9. Recently, *GDF2* (encoding BMP9) mutations have been described in three unrelated individuals presenting with a vascular anomaly syndrome with phenotypic overlap with hereditary hemorrhagic telangiectasia (8). The mutations occurred within the pro-domain and the mature peptide and were associated with a defect in BMP9 processing. Further work, including the application of ELISA measurements, is needed to show how these mutations affect circulating levels of

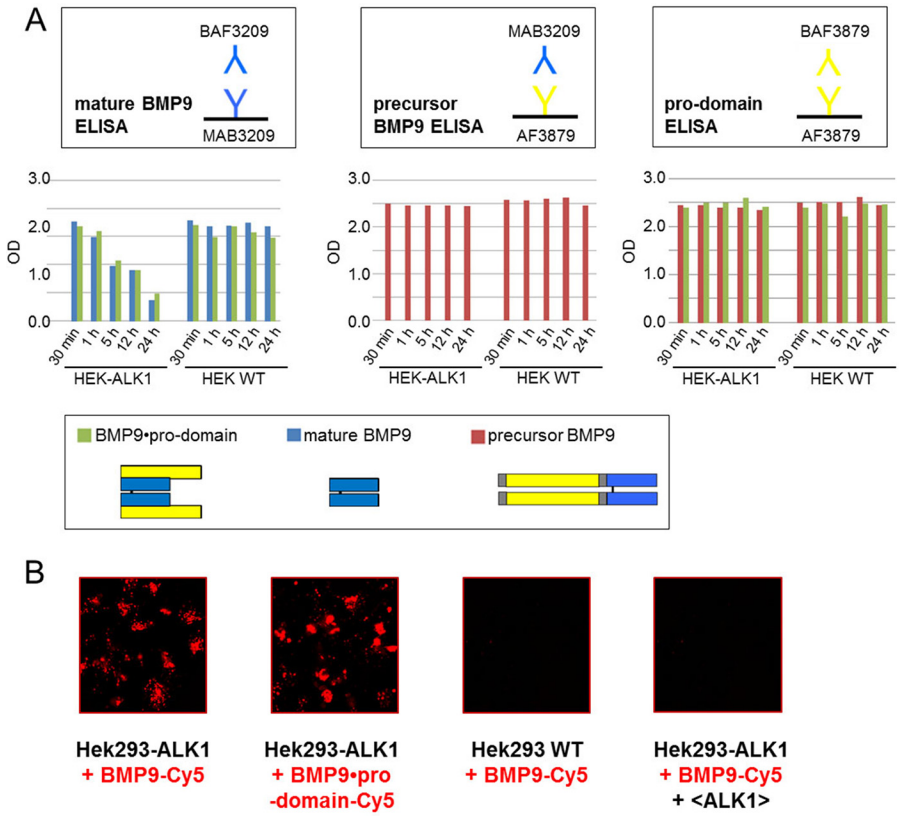

FIGURE 11. **Pro-domain release occurs also upon binding of BMP9·pro-domain to living cells.** *A*, ALK1-transfected or wild type HEK293 cells were treated with 2 nM mature BMP9, BMP9·pro-domain, and precursor BMP9. Supernatants were subjected to novel ELISA assays described above at different time points (30 min to 24 h). *B*, internalization of Cy5-labeled mature BMP9 and BMP9·pro-domain in ALK1-transfected or wild type HEK293 cells with and without anti-ALK1 antibody after 24 h.

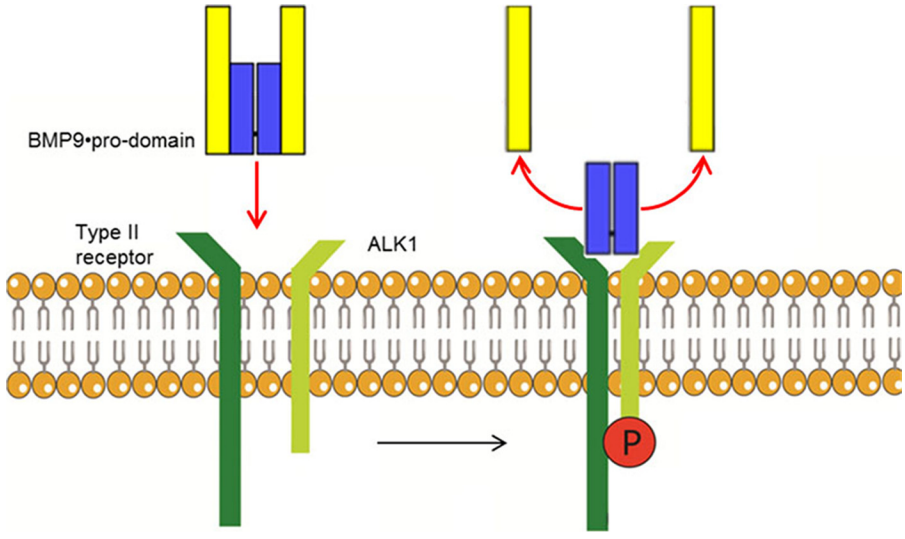

FIGURE 12. **Model for BMP9·pro-domain binding to ALK1.** ALK1 and type II receptors can rearrange the pro-domains of the BMP9·pro-domain complex *per se* and led to complete displacement of the pro-domains after receptor binding, leading to rapid activation of BMP9 signaling.

BMP9 or its signaling to ALK1 and if patients benefit from administration of BMP9.

This study has provided new insight into the activation of BMP9 and gives answers to the questions regarding the role of the pro-domains in BMP9 biology. We have presented detailed information on BMP9·pro-domain complex binding to ALK1, type II receptors BMPRII, ActRIIA, and ActRIIB as well as co-receptor ENG, demonstrating that the pro-peptide part is readily released from the mature growth factor to free the receptor binding interface, generating an active ligand. Clearly, pro-domains do not confer latency to the mature growth factor in the soluble state, and it can be speculated that they also do not target the BMP9 cytokine to the extracellular matrix or that at least BMP9 would not be retained in a stable complex there. Instead, pro-domain complexation might simply function to protect the small mature BMP9 from renal filtration (90.3 *ver-*

sus 24.2 kDa), considering that it must travel long distances from its primary production site in the liver to reach peripheral targets. Additionally, our data give essential information for the development of ELISA assays for the detection and quantification of circulating BMP9 variants for future analysis of vascular and other disorders linked to the BMP9 signaling pathway.

Author Contributions—Y. K., S. L., S. S., and C. L. conceived and coordinated the study. Y. K. and S. S. wrote the manuscript. U. J. designed, performed, and analyzed the experiments shown in Figs. 2–7. S. S. designed and analyzed the experiments shown in Figs. 2–7. M. T. and M. d W. designed, performed, and analyzed the experiments shown in Figs. 8–10. A. H. designed and constructed vectors for expression of BMP9 proteins. V. B. and D. B. provided valuable technical assistance. K. H. and Y. K. designed and analyzed the experiments shown in Fig. 11. All authors reviewed the results and approved the final version of the manuscript.

Acknowledgments—We acknowledge the valuable technical support provided (in alphabetical order) by Verena Schueck, Sabine Schuster, Annette Seidl, Ulrike Thomas, and Oliver Tonn.

References

1. Bidart, M., Ricard, N., Levet, S., Samson, M., Mallet, C., David, L., Subileau, M., Tillet, E., Feige, J. J., and Bailly, S. (2012) BMP9 is produced by hepatocytes and circulates mainly in an active mature form complexed to its prodomain. *Cell. Mol. Life Sci.* **69,** 313–324
2. David, L., Mallet, C., Keramidas, M., Lamandé, N., Gasc, J. M., Dupuis-Girod, S., Plauchu, H., Feige, J. J., and Bailly, S. (2008) Bone morphogenetic protein-9 is a circulating vascular quiescence factor. *Circ. Res.* **102,** 914–922
3. David, L., Mallet, C., Mazerbourg, S., Feige, J. J., and Bailly, S. (2007) Identification of BMP9 and BMP10 as functional activators of the orphan activin receptor-like kinase 1 (ALK1) in endothelial cells. *Blood* **109,** 1953–1961
4. Oh, S. P., Seki, T., Goss, K. A., Imamura, T., Yi, Y., Donahoe, P. K., Li, L., Miyazono, K., ten Dijke, P., Kim, S., and Li, E. (2000) Activin receptor-like kinase 1 modulates transforming growth factor-β1 signaling in the regulation of angiogenesis. *Proc. Natl. Acad. Sci. U.S.A.* **97,** 2626–2631
5. Ricard, N., Ciais, D., Levet, S., Subileau, M., Mallet, C., Zimmers, T. A., Lee, S. J., Bidart, M., Feige, J. J., and Bailly, S. (2012) BMP9 and BMP10 are critical for postnatal retinal vascular remodeling. *Blood* **119,** 6162–6171
6. Chen, H., Brady Ridgway, J., Sai, T., Lai, J., Warming, S., Chen, H., Roose-Girma, M., Zhang, G., Shou, W., and Yan, M. (2013) Context-dependent signaling defines roles of BMP9 and BMP10 in embryonic and postnatal development. *Proc. Natl. Acad. Sci. U.S.A.* **110,** 11887–11892
7. Johnson, D. W., Berg, J. N., Baldwin, M. A., Gallione, C. J., Marondel, I., Yoon, S. J., Stenzel, T. T., Speer, M., Pericak-Vance, M. A., Diamond, A., Guttmacher, A. E., Jackson, C. E., Attisano, L., Kucherlapati, R., Porteous, M. E., and Marchuk, D. A. (1996) Mutations in the activin receptor-like kinase 1 gene in hereditary hemorrhagic telangiectasia type 2. *Nat. Genet.* **13,** 189–195
8. Wooderchak-Donahue, W. L., McDonald, J., O'Fallon, B., Upton, P. D., Li, W., Roman, B. L., Young, S., Plant, P., Fülöp, G. T., Langa, C., Morrell, N. W., Botella, L. M., Bernabeu, C., Stevenson, D. A., Runo, J. R., and Bayrak-Toydemir, P. (2013) BMP9 mutations cause a vascular-anomaly syndrome with phenotypic overlap with hereditary hemorrhagic telangiectasia. *Am. J. Hum. Genet.* **93,** 530–537
9. López-Coviella, I., Berse, B., Krauss, R., Thies, R. S., and Blusztajn, J. K. (2000) Induction and maintenance of the neuronal cholinergic phenotype in the central nervous system by BMP-9. *Science* **289,** 313–316
10. Cheng, H., Jiang, W., Phillips, F. M., Haydon, R. C., Peng, Y., Zhou, L., Luu, H. H., An, N., Breyer, B., Vanichakarn, P., Szatkowski, J. P., Park, J. Y., and He, T. C. (2003) Osteogenic activity of the fourteen types of human bone morphogenetic proteins (BMPs). *J. Bone Joint Surg. Am.* **85,** 1544–1552
11. Kang, Q., Song, W. X., Luo, Q., Tang, N., Luo, J., Luo, X., Chen, J., Bi, Y., He, B. C., Park, J. K., Jiang, W., Tang, Y., Huang, J., Su, Y., Zhu, G. H., He, Y., Yin, H., Hu, Z., Wang, Y., Chen, L., Zuo, G. W., Pan, X., Shen, J., Vokes, T., Reid, R. R., Haydon, R. C., Luu, H. H., and He, T. C. (2009) A comprehensive analysis of the dual roles of BMPs in regulating adipogenic and osteogenic differentiation of mesenchymal progenitor cells. *Stem Cells Dev.* **18,** 545–559
12. Luo, J., Tang, M., Huang, J., He, B. C., Gao, J. L., Chen, L., Zuo, G. W., Zhang, W., Luo, Q., Shi, Q., Zhang, B. Q., Bi, Y., Luo, X., Jiang, W., Su, Y., Shen, J., Kim, S. H., Huang, E., Gao, Y., Zhou, J. Z., Yang, K., Luu, H. H., Pan, X., Haydon, R. C., Deng, Z. L., and He, T. C. (2010) TGFβ/BMP type I receptors ALK1 and ALK2 are essential for BMP9-induced osteogenic signaling in mesenchymal stem cells. *J. Biol. Chem.* **285,** 29588–29598
13. Townson, S. A., Martinez-Hackert, E., Greppi, C., Lowden, P., Sako, D., Liu, J., Ucran, J. A., Liharska, K., Underwood, K. W., Seehra, J., Kumar, R., and Grinberg, A. V. (2012) Specificity and structure of a high affinity activin receptor-like kinase 1 (ALK1) signaling complex. *J. Biol. Chem.* **287,** 27313–27325
14. Scharpfenecker, M., van Dinther, M., Liu, Z., van Bezooijen, R. L., Zhao, Q., Pukac, L., Löwik, C. W., and ten Dijke, P. (2007) BMP-9 signals via ALK1 and inhibits bFGF-induced endothelial cell proliferation and VEGF-stimulated angiogenesis. *J. Cell Sci.* **120,** 964–972
15. Shi, M., Zhu, J., Wang, R., Chen, X., Mi, L., Walz, T., and Springer, T. A. (2011) Latent TGF-β structure and activation. *Nature* **474,** 343–349
16. Sengle, G., Ono, R. N., Sasaki, T., and Sakai, L. Y. (2011) Prodomains of transforming growth factor β (TGFβ) superfamily members specify different functions: extracellular matrix interactions and growth factor bioavailability. *J. Biol. Chem.* **286,** 5087–5099
17. Sengle, G., Charbonneau, N. L., Ono, R. N., Sasaki, T., Alvarez, J., Keene, D. R., Bächinger, H. P., and Sakai, L. Y. (2008) Targeting of bone morphogenetic protein growth factor complexes to fibrillin. *J. Biol. Chem.* **283,** 13874–13888
18. Crawford, S. E., Stellmach, V., Murphy-Ullrich, J. E., Ribeiro, S. M., Lawler, J., Hynes, R. O., Boivin, G. P., and Bouck, N. (1998) Thrombospondin-1 is a major activator of TGF-β1 *in vivo*. *Cell* **93,** 1159–1170
19. Munger, J. S., Huang, X., Kawakatsu, H., Griffiths, M. J., Dalton, S. L., Wu, J., Pittet, J. F., Kaminski, N., Garat, C., Matthay, M. A., Rifkin, D. B., and Sheppard, D. (1999) The integrin alpha v β 6 binds and activates latent TGF β 1: a mechanism for regulating pulmonary inflammation and fibrosis. *Cell* **96,** 319–328
20. Lyons, R. M., Keski-Oja, J., and Moses, H. L. (1988) Proteolytic activation of latent transforming growth factor-β from fibroblast-conditioned medium. *J. Cell Biol.* **106,** 1659–1665
21. Brown, M. A., Zhao, Q., Baker, K. A., Naik, C., Chen, C., Pukac, L., Singh, M., Tsareva, T., Parice, Y., Mahoney, A., Roschke, V., Sanyal, I., and Choe, S. (2005) Crystal structure of BMP-9 and functional interactions with pro-region and receptors. *J. Biol. Chem.* **280,** 25111–25118
22. Mi, L. Z., Brown, C. T., Gao, Y., Tian, Y., Le, V. Q., Walz, T., and Springer, T. A. (2015) Structure of bone morphogenetic protein 9 procomplex. *Proc. Natl. Acad. Sci. U.S.A.* **112,** 3710–3715
23. Hu-Lowe, D. D., Chen, E., Zhang, L., Watson, K. D., Mancuso, P., Lappin, P., Wickman, G., Chen, J. H., Wang, J., Jiang, X., Amundson, K., Simon, R., Erbersdobler, A., Bergqvist, S., Feng, Z., Swanson, T. A., Simmons, B. H., Lippincott, J., Casperson, G. F., Levin, W. J., Stampino, C. G., Shalinsky, D. R., Ferrara, K. W., Fiedler, W., and Bertolini, F. (2011) Targeting activin receptor-like kinase 1 inhibits angiogenesis and tumorigenesis through a mechanism of action complementary to anti-VEGF therapies. *Cancer Res.* **71,** 1362–1373
24. Mitchell, D., Pobre, E. G., Mulivor, A. W., Grinberg, A. V., Castonguay, R., Monnell, T. E., Solban, N., Ucran, J. A., Pearsall, R. S., Underwood, K. W., Seehra, J., and Kumar, R. (2010) ALK1-Fc inhibits multiple mediators of angiogenesis and suppresses tumor growth. *Mol. Cancer Ther.* **9,** 379–388
25. Castonguay, R., Werner, E. D., Matthews, R. G., Presman, E., Mulivor, A. W., Solban, N., Sako, D., Pearsall, R. S., Underwood, K. W., Seehra, J., Kumar, R., and Grinberg, A. V. (2011) Soluble endoglin specifically binds bone morphogenetic proteins 9 and 10 via its orphan domain, inhibits blood vessel formation, and suppresses tumor growth. *J. Biol. Chem.* **286,**

30034–30046
26. Sengle, G., Ono, R. N., Lyons, K. M., Bächinger, H. P., and Sakai, L. Y. (2008) A new model for growth factor activation: type II receptors compete with the prodomain for BMP-7. *J. Mol. Biol.* **381,** 1025–1039
27. Hauburger, A., von Einem, S., Schwaerzer, G. K., Buttstedt, A., Zebisch, M., Schräml, M., Hortschansky, P., Knaus, P., and Schwarz, E. (2009) The pro-form of BMP-2 interferes with BMP-2 signalling by competing with BMP-2 for IA receptor binding. *FEBS J.* **276,** 6386–6398
28. Gregory, K. E., Ono, R. N., Charbonneau, N. L., Kuo, C. L., Keene, D. R., Bächinger, H. P., and Sakai, L. Y. (2005) The prodomain of BMP-7 targets the BMP-7 complex to the extracellular matrix. *J. Biol. Chem.* **280,** 27970–27980
29. Ramirez, F., and Rifkin, D. B. (2009) Extracellular microfibrils: contextual platforms for TGFβ and BMP signaling. *Curr. Opin. Cell Biol.* **21,** 616–622
30. Ramirez, F., and Sakai, L. Y. (2010) Biogenesis and function of fibrillin assemblies. *Cell Tissue Res.* **339,** 71–82
31. Hintze, V., Samsonov, S. A., Anselmi, M., Moeller, S., Becher, J., Schnabelrauch, M., Scharnweber, D., and Pisabarro, M. T. (2014) Sulfated glycosaminoglycans exploit the conformational plasticity of bone morphogenetic protein-2 (BMP-2) and alter the interaction profile with its receptor. *Biomacromolecules* **15,** 3083–3092
32. Hintze, V., Miron, A., Moeller, S., Schnabelrauch, M., Wiesmann, H. P., Worch, H., and Scharnweber, D. (2012) Sulfated hyaluronan and chondroitin sulfate derivatives interact differently with human transforming growth factor-β1 (TGF-β1). *Acta Biomater.* **8,** 2144–2152
33. Jiang, H., Salmon, R. M., Upton, P. D., Wei, Z., Lawera, A., Davenport, A. P., Morrell, N. W., and Li, W. (2015) The prodomain-bound form of bone morphogenetic protein 10 is biologically active on endothelial cells. *J. Biol. Chem.* **290,** in press
34. Herrera, B., and Inman, G. J. (2009) A rapid and sensitive bioassay for the simultaneous measurement of multiple bone morphogenetic proteins: identification and quantification of BMP4, BMP6 and BMP9 in bovine and human serum. *BMC. Cell Biol.* **10,** 20
35. Wei, Z., Salmon, R. M., Upton, P. D., Morrell, N. W., and Li, W. (2014) Regulation of bone morphogenetic protein 9 (BMP9) by redox-dependent proteolysis. *J. Biol. Chem.* **289,** 31150–31159
36. Luther, G., Wagner, E. R., Zhu, G., Kang, Q., Luo, Q., Lamplot, J., Bi, Y., Luo, X., Luo, J., Teven, C., Shi, Q., Kim, S. H., Gao, J. L., Huang, E., Yang, K., Rames, R., Liu, X., Li, M., Hu, N., Liu, H., Su, Y., Chen, L., He, B. C., Zuo, G. W., Deng, Z. L., Reid, R. R., Luu, H. H., Haydon, R. C., and He, T. C. (2011) BMP-9 induced osteogenic differentiation of mesenchymal stem cells: molecular mechanism and therapeutic potential. *Curr. Gene Ther.* **11,** 229–240
37. Burke, R. M., Norman, T. A., Haydar, T. F., Slack, B. E., Leeman, S. E., Blusztajn, J. K., and Mellott, T. J. (2013) BMP9 ameliorates amyloidosis and the cholinergic defect in a mouse model of Alzheimer's disease. *Proc. Natl. Acad. Sci. U.S.A.* **110,** 19567–19572
38. Cunha, S. I., Pardali, E., Thorikay, M., Anderberg, C., Hawinkels, L., Goumans, M. J., Seehra, J., Heldin, C. H., ten Dijke, P., and Pietras, K. (2010) Genetic and pharmacological targeting of activin receptor-like kinase 1 impairs tumor growth and angiogenesis. *J. Exp. Med.* **207,** 85–100